Research Square

Preprints are preliminary reports that have not undergone peer review.
They should not be considered conclusive, used to inform clinical practice,
or referenced by the media as validated information.

Individualized Acetabular Cup Placement Strategy Constrained by Seated Combined Anteversion in Patients with Spinopelvic Rigidity

Yuan Gao
Guizhou Hospital of Beijing Jishuitan Hospital
Liliang Chen
Affiliated Hospital of Guizhou Medical University
Feng Pan
Guizhou Hospital of Beijing Jishuitan Hospital
Desu Luo
Guizhou Hospital of Beijing Jishuitan Hospital
Kunzhi Zhu
Guizhou Hospital of Beijing Jishuitan Hospital
Jun Zhang
Guizhou Hospital of Beijing Jishuitan Hospital
Songjie Ji
jisongjie@gmail.com

Beijing Jishuitan Hospital, Capital Medical University

Research Article

Keywords: Arthroplasty Replacement Hip, Mixed Reality, Spinopelvic Kinematics, Femoral Functional Anteversion, Seated Combined Anteversion

Posted Date: November 12th, 2026

DOI: https://doi.org/10.21203/rs.3.rs-11385159/v1

License: This work is licensed under a Creative Commons Attribution 4.0 International License. Read Full License

Additional Declarations: No competing interests reported.

Abstract

Background

The conventional static Lewinnek safe zone does not account for the functional change in cup position produced by standing-to-sitting pelvic tilt, and individualized cup placement strategies for patients with spinopelvic rigidity are lacking. We therefore evaluated an individualized total hip arthroplasty (THA) strategy in such patients, using seated functional femoral anteversion (FFA_sit) as a fixed baseline and a seated combined anteversion (CA_sit) of 45–65° as a rigid constraint.

Methods

This prospective single-arm case series enrolled 15 patients (5 men and 10 women; mean age 63.5 ± 8.6 years) undergoing primary THA between January 2019 and January 2024. Preoperative computed tomography (CT) and standing and seated EOS biplanar imaging were imported into a mixed-reality (MR) planning system. With FFA_sit fixed, acetabular abduction and anteversion were iteratively adjusted, with CA_sit as the primary constraint, together with freedom from seated impingement, adequate standing range of motion and standing functional acetabular abduction ≤ 45°. Surgery was performed under MR navigation. The primary outcome was the mean absolute error (MAE) between the MR-planned and the postoperative CT-measured anatomical acetabular anteversion (RA).

Results

The MAE for RA was 1.68°, and the mean CA_sit was 51.8° ± 2.8°, with no prosthetic impingement. Planned RA ranged from 26° to 35°, above the conventional static target of RA = 20° in the same anatomical coordinate system. Preoperative simulation indicated that 46.7% of patients were incompatible with a uniform RA = 20° protocol and that 33.3% could not satisfy all seated functional constraints within the conventional safe-zone anteversion range (simulation, not clinical, results). At 14.2 ± 2.5 months, Harris and Oxford scores improved significantly (both $P < 0.001$), with no dislocation or impingement.

Conclusions

This dual-position individualized strategy achieved satisfactory angular reproducibility of cup placement, and simulation suggests that the conventional static safe zone inadequately covers the seated functional anteversion requirements of these patients. Short-term outcomes were reliable. As a single-centre, single-arm case series (level IV evidence), the study can evaluate feasibility only and cannot establish superiority over conventional techniques.

Introduction

Total hip arthroplasty (THA) is the mainstay treatment for end-stage hip disease, and the spatial orientation of the acetabular cup directly determines postoperative joint stability, prosthetic impingement, and polyethylene (PE) wear risk. The static Lewinnek safe zone (abduction 30°–50°, anteversion 5°–25°) has long been used

clinically to guide cup placement[1]; however, this safe zone was established from static pelvic imaging and cannot reflect the functional changes in cup position caused by pelvic postural change during standing-to-sitting transitions.[2, 3]

Some patients after lumbar spinal fusion, or with ankylosing spondylitis or severe lumbar degeneration, have restricted pelvic mobility from standing to sitting. They may be unable to increase functional acetabular anteversion through seated posterior pelvic tilt, and even when the static cup position lies within the conventional reference range, seated impingement and instability may still occur.[4–7] Beyond pelvic factors, femoral axial rotation can also change with functional posture; therefore, anteversion defined by local femoral anatomical landmarks is not equivalent to functional anteversion relative to an external reference frame. As reported by Hardwick-Morris et al.[8], 46% of patients had spontaneous femoral axial rotation > 10° and 16% had standing functional femoral anteversion (FFA_st) > 25°, indicating a significant discrepancy between anatomical and functional anteversion. Seated combined anteversion is defined as the sum of seated functional acetabular anteversion and seated functional femoral anteversion; it integrates both pelvic and femoral factors to assess prosthetic impingement risk in the seated hip-flexed internal-rotation position. In addition, a standing functional acetabular abduction angle > 45° markedly increases liner edge loading and accelerates prosthetic wear, and must therefore be treated as a mechanical constraint.[9]

In summary, there is a need to explore a dual-position cup planning and implementation workflow suitable for patients with spinopelvic rigidity. Accordingly, this study proposes an individualized acetabular placement strategy constrained by seated combined anteversion, using the preoperatively measured seated functional femoral anteversion (FFA_sit) as a fixed baseline and 45°–65° seated combined anteversion as a rigid constraint, combined with an MR navigation system to assist in screening individualized target cup angles and guide precise implantation. In this exploratory feasibility study, the primary outcome was the accuracy of angular transfer from plan to implant, defined as the mean absolute error (MAE) between the MR-planned and the postoperative CT-measured anatomical acetabular anteversion (RA). Reduction of prosthesis-related complications was not a primary outcome. The study aimed to preliminarily evaluate the feasibility and short-term efficacy of this strategy in complex THA for patients with spinopelvic rigidity.

Methods

Inclusion and exclusion criteria

Inclusion criteria: (a) diagnosis of spinopelvic rigidity, i.e., previous lumbar spinal fusion, ankylosing spondylitis with bony ankylosis, or severe lumbar degeneration (radiologically confirmed extensive degeneration causing restricted mobility); (b) standing-to-seated pelvic tilt change (ΔPT) < 10°; (c) indication for primary THA and consent to MR-navigated surgery; and (d) complete data with a follow-up of at least 12 months.

Exclusion criteria: (a) active or previous hip joint infection; (b) revision THA; (c) severe proximal femoral deformity or a history of osteotomy or prosthesis implantation that could affect measurement of femoral anteversion; and (d) incomplete clinical or imaging data, or follow-up of less than 12 months.

General data

This single-center case series was approved by the Ethics Committee of Guizhou Hospital of Beijing Jishuitan Hospital (approval No. KT2019011001). The study was conducted in accordance with the Declaration of Helsinki and its subsequent amendments, and all patients provided written informed consent. As an exploratory feasibility study that did not aim to test efficacy hypotheses, no a priori sample size calculation was performed; all consecutive patients meeting the inclusion and exclusion criteria during the study period were enrolled. A total of 15 patients were enrolled between January 2019 and January 2024, including 5 men and 10 women, with a mean age of 63.5 ± 8.6 years (range, 48–78 years) and a mean BMI of 24.6 ± 3.2 kg/m²; the affected hip was on the left in 6 patients and on the right in 9. Spinal conditions included previous lumbar spinal fusion in 7 patients, ankylosing spondylitis in 3, and severe lumbar degeneration in 5. The mean ΔPT was 1.9° ± 0.2° (range, 1.5°–2.3°), and the mean seated functional femoral anteversion (FFA_sit) was 18.3° ± 4.7° (range, 10.5°–25.5°). Femoral head size was 28 mm in 1 patient, 32 mm in 9, and 36 mm in 5. The mean preoperative Harris score was 48.6 ± 10.2 and the Oxford score 22.3 ± 6.8; all patients were followed up for 14.2 ± 2.5 months, and the follow-up duration was ≥ 12 months in every case.

Study methods

Preoperative imaging data acquisition and parameter measurement

(1) Imaging protocol

1. (a) Supine full-length CT of the pelvis and femur: from the upper margin of the ilium to the distal femur, slice thickness 0.625 mm; anatomical femoral anteversion (AFA) and supine pelvic tilt (PT_sup) were measured, and bony contours were extracted for MR registration.
2. (b) Standing and seated EOS biplanar imaging: performed in the natural standing position and the standard seated position (hip and knee flexed approximately 90°). Three-dimensional models of both positions were reconstructed, pelvic tilt and functional femoral rotation (FFR) were measured, and ΔPT as well as FFA_sit and FFA_st were calculated.

(2) Parameter definitions and calculation standards

1. (a) Functional femoral rotation (FFR): axial rotation of the femoral posterior condylar axis relative to the coronal plane in a functional posture, measured from the EOS three-dimensional reconstruction[8]; internal rotation is recorded as positive and external rotation as negative, denoted FFR-st and FFR-se.
2. (b) Functional femoral anteversion (FFA): FFA = AFA + FFR in the same posture, where AFA was obtained from supine CT. The seated FFA_sit served as the fixed femoral baseline and remained unchanged throughout screening.
3. (c) Acetabular angles: anatomical acetabular abduction (RI) and anatomical acetabular anteversion (RA) are defined in the pelvic anatomical coordinate system; they are the target angles output by MR navigation and executed intraoperatively, and postoperative CT measurement of RA used the same coordinate system. Seated functional acetabular anteversion (FA_sit), seated functional acetabular abduction (FI_sit), and standing functional acetabular abduction (FI_st) were measured directly from the EOS three-dimensional

reconstruction; because seated posterior pelvic tilt is restricted, FI_sit and FI_st had to be measured separately.

4. (d) Combined anteversion and thresholds: seated combined anteversion (CA_sit) = FA_sit + FFA_sit was a rigid constraint that had to be satisfied during screening, where FA_sit and FFA_sit are the seated functional acetabular anteversion and the seated functional femoral anteversion of the operated hip, respectively; standing combined anteversion (CA_st) = FA_st + FFA_st was used for postural offset analysis, where FA_st and FFA_st are the corresponding standing values, and FI_st ≤ 45° was the standing edge-loading safety threshold. The 45°–65° CA_sit range was determined from the virtual range-of-motion simulation study by O'Connor et al.[9], in which more than 99% of simulations within this range achieved an impingement-free range of motion; that study also proposed 30°–50° standing combined anteversion as an impingement-free reference range. In the present study, seated combined anteversion served as the rigid constraint while standing combined anteversion was used only as an auxiliary verification index. This threshold represents an exploratory cut-off derived from in vitro virtual simulation; it has not been validated in large clinical cohorts and is not an accepted gold-standard reference.

(3) Prosthesis parameters

All patients received a Corail straight stem (DePuy Synthes, USA; neck-shaft angle 135°) combined with a PINNACLE hemispherical acetabular cup and a 28–36 mm femoral head. The actual prosthesis model, size, neck-shaft angle, neck length, and liner geometry of each case were imported into the planning system for range-of-motion and impingement simulation (Fig. 1).

(4) Measurement quality control

Imaging parameters were measured independently by 2 senior orthopedic surgeons blinded to each other's results, with 2 repeated measurements per parameter set at a 7-day interval, using a two-way random-effects, absolute-agreement model: the intra-observer intraclass correlation coefficient (ICC) for preoperative imaging parameters was 0.92–0.96 and the inter-observer ICC 0.88–0.92 (parameter-specific values for the anatomical angles are given in Section 1.3.2), indicating good reproducibility; intra- and inter-observer ICCs for postoperative CT-measured RA were 0.92 and 0.88, respectively, comparable to preoperative values. The mean of the repeated measurements by the 2 observers was used for statistical analysis.

Individualized angle screening workflow constrained by seated combined anteversion

The MR system consisted of a Microsoft HoloLens 2 headset (Smart Vision HipArthro-VR) and Hip Planning 3.0 planning software (Shenzhen Yitu Intelligent Technology Co., Ltd.), with registration performed using iterative closest point (ICP) point-cloud registration based on bony surface contours. After importing the three-dimensional model, spinopelvic parameters, FFA_sit, and prosthetic geometry, target angles were screened through model registration, dual-position posture reproduction, and prosthetic motion simulation. All simulations were based on bony three-dimensional models and did not incorporate soft-tissue tension (muscle, capsule) or patient-reported symptoms; they therefore cannot replace intraoperative stability testing.

(1) Three-dimensional model registration and virtual-real fusion

Using pelvic and femoral surface point clouds as references, the supine CT bony model was registered to the standing and seated EOS three-dimensional coordinate systems using the ICP algorithm. Registration performance was evaluated by repeated calibration-sphere tests (n = 10) and comparison with clinical bony point clouds from 5 cases: target registration error (TRE) ≤ 1.5 mm and rotational residual ≤ 1.0° (maximum error). These values represent bench-test and offline point-cloud results rather than per-case intraoperative real-time registration error. FA_sit and FFA_sit share the seated EOS coordinate system, and an error in the orientation of the coordinate system shifts both parameters in the same direction: if the two errors are fully correlated, the deviation in CA_sit may be twice that of a single parameter (conservative upper bound, ≤ 2.0°); if they are independent, the root-sum-square combination is approximately √2 ≈ 1.4 times the single-parameter error. In this cohort the minimum margin of CA_sit from the target interval boundary was 2.8°; an error of this magnitude could push borderline cases outside the interval, so a safety margin was applied during preoperative planning for cases with insufficient margin.

(2) Candidate acetabular cup angle setting and traversal strategy

Preoperative anatomical RI and RA were measured on the CT/EOS three-dimensional models of each case as individualized reference values (2 observers, 2 measurements each; inter-observer ICC 0.908 for RI with a standard error of measurement (SEM) of 0.43°, and 0.883 for RA with an SEM of 0.64°); the mean of the 4 measurements was used to judge anatomical proximity when candidates were tied.

1. (a) Coarse screening and local refinement: RI ranged from 30° to 50° and RA from 0° to 35° in 5° steps, giving 40 initial candidates. When a candidate approached the CA_sit boundary, refined traversal was performed with the qualifying point as the center, extending RI and RA by ± 5° in 1° steps (121 combinations per point), with overlapping neighborhoods evaluated only once. The proportion of evaluated candidates that passed was defined as the number of candidates satisfying all conditions divided by the total number of independent candidates evaluated for that case.
2. (b) Postural angle conversion: each RI/RA pair was assigned to the cup model in the pelvic coordinate system, FA_sit and FI_st were measured directly from the seated and standing EOS three-dimensional models, and CA_sit was calculated as FA_sit + FFA_sit.

(3) Position-specific dynamic simulation validation and optimal angle selection

(a) Screening criteria: with FFA_sit fixed, all candidates were traversed and checked sequentially: (i) avoidance of seated impingement, i.e., no model-defined component or bony impingement at 90° hip flexion with 30° internal rotation; (ii) CA_sit within 45°–65°; (iii) standing maximum flexion ≥ 110° and maximum extension ≥ 20°, with no component interference and a minimum clearance of ≥ 1 mm throughout the range of flexion and extension; and (iv) FI_st ≤ 45° (Table 1).

Table 1
Preoperative planning parameters and seated combined anteversion (n = 15)

No.	FFA_sit (°)	RI (°)	Preop anatomical RI (°)	RA (°)	Preop anatomical RA (°)	PT_st (°)	PT_sit (°)	ΔPT (°)	FA_sit (°)	CA_sit (°)
1	14.5	35	35.5	31	30.2	11.2	13.1	1.9	35.7	50.2
2	22.3	38	38.0	26	24.9	14.4	16.3	1.9	32.3	54.6
3	11.2	35	35.5	34	33.0	8.7	10.4	1.7	37.5	48.7
4	25.5	40	40.1	27	26.2	15.1	17.4	2.3	30.6	56.1
5	18.7	36	36.5	28	27.2	11.8	13.6	1.8	32.6	51.3
6	15.2	37	37.0	30	28.8	10.5	12.2	1.7	34.3	49.5
7	23.8	39	39.2	27	26.3	14.7	16.8	2.1	31.6	55.4
8	10.5	34	34.1	35	34.4	7.9	9.4	1.5	37.3	47.8
9	20.1	38	38.3	28	27.0	12.6	14.5	1.9	32.6	52.7
10	17.3	37	37.0	29	28.4	11.1	12.9	1.8	33.1	50.4
11	13.6	38	37.6	32	31.4	9.8	11.4	1.6	35.5	49.1
12	24.2	40	40.2	28	27.2	14.6	16.9	2.3	31.6	55.8
13	16.4	38	38.5	29	28.2	10.9	12.7	1.8	33.4	49.8
14	19.5	39	39.0	29	28.1	12.3	14.2	1.9	32.7	52.2
15	21.8	41	41.0	28	26.8	13.5	15.7	2.2	32.1	53.9
Mean ± SD	18.3 ± 4.7	37.7 ± 2.0	37.8 ± 1.9	29.4 ± 2.6	28.5 ± 2.7	11.9 ± 2.2	13.8 ± 2.4	1.9 ± 0.2	33.5 ± 2.1	51.8 ± 2.8

Note: FFA_sit, seated functional femoral anteversion; RI and RA, anatomical target angles directly guided by MR navigation (anatomical abduction and anatomical anteversion); FA_sit, seated functional acetabular anteversion; CA_sit, seated combined anteversion = FA_sit measured from the seated EOS three-dimensional model + seated FFA_sit; PT_st and PT_sit, standing and seated pelvic tilt, ΔPT = PT_sit − PT_st; preoperative anatomical RI/RA were measured along the native acetabular rim plane and represent the mean of two measurements per observer by each of two observers (four measurements in total).

1. (b) Optimal angle selection: solutions satisfying all constraints were considered feasible; among them the one with the smallest FI_st was selected first, and ties were broken in order by the smallest |RI − preoperative anatomical RI|, the smallest |RA − preoperative anatomical RA|, the smaller RA, and the smaller RI, so that the optimal solution was unique. If the feasible solution space was empty, the FI_st and range-of-motion thresholds were relaxed sequentially and traversal was repeated; the feasible solution space was not empty in any of the 15 cases, so no threshold relaxation was required.
2. (c) Prespecified secondary analyses (defined before analysis and not used for inference on the primary endpoint): (i) no conventional safe-zone fit (exploratory): the feasible solution space was searched for a solution in which the anatomical RA and anatomical RI both fell within the numerical limits of the Lewinnek safe zone (anteversion 5°–25°, abduction 30°–50°), and the absence of such a solution was judged as no

fit. Importantly, RA/RI in this study are anatomical CT-based angles whereas the Lewinnek safe zone is defined radiologically on anteroposterior pelvic radiographs, and the two cannot be quantitatively converted; this endpoint therefore applies no coordinate conversion and instead reads the safe-zone numerical limits within a single (anatomical) coordinate system. Its result is not equivalent to a radiological safe-zone assessment: because, under the standard anatomical definitions, the anatomical anteversion of a given cup orientation is numerically larger than its radiological anteversion, this reading is more stringent than a radiological test in the anteversion dimension, and the proportion of non-fit reported here is therefore used only as an exploratory, conservative qualitative comparison and not to infer the true radiological safe-zone non-conformity rate. (ii) incompatibility with the standardized protocol: RA was fixed at 20° with all other parameters unchanged, FA_sit was converted according to the linear relationship between RA and FA_sit in each case (FA_sit = 0.771 × RA + 10.87, r = 0.952), CA_sit was calculated, and a value < 45° was judged as incompatible.

Surgical procedure

All procedures were performed by the same surgical team using a standardized posterolateral approach. The MR navigation system was activated intraoperatively, and the individualized optimal RI/RA (anatomical angles) screened preoperatively by dual-position dynamic simulation under the seated combined anteversion constraint were superimposed in real time on the surgical field as semi-transparent virtual overlays to guide precise cup placement. A Corail cementless stem was implanted in all cases according to the standard technique. After initial cup placement, the actual implanted anatomical RI and RA (i.e., angles defined in the anatomical, not the functional, posture) were immediately verified by navigation, and the cup was repositioned if the error between planned and measured angles exceeded 3°. After implantation of all components, the hip was passively moved through its full range intraoperatively to check joint stability and range of motion, with particular attention to impingement during hip flexion with internal rotation and hip extension with external rotation, after which the wound was closed layer by layer. All procedures were performed under general or spinal anesthesia.

Statistical methods

SPSS 26.0 (IBM Corp., Armonk, NY, USA) was used for analysis and GraphPad Prism 9.5 for plotting. Quantitative data are expressed as mean ± standard deviation. The Shapiro-Wilk test was used to assess normality of each variable and of the paired differences d, where d = postoperative CT-measured RA − MR-planned RA. Intra- and inter-observer agreement was assessed with ICC(2,1) and the SEM was calculated (the mean of 2 repeated measurements by each of 2 observers was used in the analysis, which is more reliable than a single measurement). The MAE was calculated with postoperative CT measurements as the reference, and Bland-Altman analysis was used to assess agreement between planned and measured RA, reporting the mean difference, 95% confidence interval (CI), and 95% limits of agreement (LoA); because d deviated from normality, MAE served as the primary accuracy metric. The relationship between the difference d and the mean of the two methods was tested by Pearson correlation, and the combined anteversion offset between the two positions was displayed as a paired difference plot. Paired t-tests were used for paired comparisons, and a one-sided 95% CI upper limit was reported for zero event rates (Clopper-Pearson exact method); other tests were two-sided. The significance level was $\alpha = 0.05$, and $P < 0.05$ was considered statistically significant.

Results

General surgical findings

All 15 patients completed surgery successfully with no intraoperative complications. The mean operative time was 78.5 ± 12.3 min, including a mean MR navigation registration time of 8.2 ± 2.1 min. The mean intraoperative blood loss was 310 ± 85 mL, and no patient received allogeneic transfusion. The intraoperative error between planned and actual implantation angles was within 3° in all cases, and no cup required repositioning because the error exceeded the preset threshold. A representative case is shown in (Fig. 2).

Accuracy of cup placement under mixed-reality navigation and quantitative assessment of edge loading

Postoperative three-dimensional CT reconstruction was used to assess placement accuracy and standing functional abduction (Table 2). The MAE between MR-planned and postoperative CT-measured RA in the 15 patients was 1.68°, and the difference was negative in 12 of the 15 cases, indicating that the implanted RA was slightly smaller than planned. The standing functional acetabular abduction angle was 34.5° ± 2.0° (range, 32°–39.9°), and all values were ≤ 45°.

Table 2
Accuracy of acetabular prosthesis placement under MR navigation and standing functional abduction (n = 15)

No.	Postop CT-measured RA (°)	Difference d (°)	Absolute error of difference d (°)	FI_st (°)
1	30.0	−1.0	1.0	39.9
2	26.2	+ 0.2	0.2	32.0
3	32.2	−1.8	1.8	33.0
4	27.8	+ 0.8	0.8	35.0
5	25.8	−2.2	2.2	36.0
6	28.0	−2.0	2.0	35.0
7	28.8	+ 1.8	1.8	33.0
8	32.4	−2.6	2.6	36.0
9	25.8	−2.2	2.2	33.0
10	27.0	−2.0	2.0	34.0
11	29.5	−2.5	2.5	35.0
12	26.2	−1.8	1.8	36.0
13	28.5	−0.5	0.5	34.0
14	27.0	−2.0	2.0	33.0
15	26.2	−1.8	1.8	33.0
Mean ± SD	28.1 ± 2.2	−1.31 ± 1.31	1.68 ± 0.72	34.5 ± 2.0

Note: RA, anatomical acetabular anteversion; FI_st, standing functional acetabular abduction, measured directly from the standing EOS three-dimensional reconstruction; the difference is defined as d = postoperative CT-measured RA − MR-planned RA; MAE, mean absolute error; standard deviations are sample standard deviations (denominator n − 1); FI_st was ≤ 45° in all 15 patients, satisfying the standing mechanical safety threshold.

Planned-measured agreement and postural offset analysis

Paired t-test between preoperative anatomical RA (28.5° ± 2.7°) and MR-planned RA (29.4° ± 2.6°) showed that MR-planned RA was significantly increased (difference 0.86° ± 0.2°, t = 16.36, P < 0.001), reflecting the individualized adjustment made to satisfy the seated combined anteversion constraint.

Because the planned-measured difference d deviated from normality (Shapiro-Wilk W = 0.821, P = 0.007), the Bland-Altman plot was presented for visual reference only and the MAE served as the primary accuracy metric in this study. Bland-Altman agreement analysis was performed with postoperative CT-measured RA as the reference (Fig. 3), where d = postoperative CT-measured RA − MR-planned RA: mean difference, − 1.31° (95% CI, − 2.03° to − 0.58°); SD of the differences (SDd), 1.31°; and 95% LoA, − 3.87° to + 1.26°; only case 7 (+ 1.80°) slightly exceeded the upper limit, and the absolute error was < 3° in all cases. Pearson correlation between the

difference d and the mean of the two methods was r = − 0.335 (P = 0.222; Spearman ρ = −0.227, P = 0.416), showing no obvious proportional bias, although the power was limited with n = 15.

The postural offset of combined anteversion between the two positions is shown as a paired difference plot (Fig. 4). All offsets were negative, with a mean of − 12.6° and no outliers, indicating that seated combined anteversion was consistently higher than standing combined anteversion, and that a single static cup position plan cannot adequately address functional safety in both positions. Paired t-test between standing combined anteversion (39.2° ± 2.1°) and seated combined anteversion (51.8° ± 2.8°) gave a mean difference of − 12.6° ± 1.01° (95% CI, − 13.16° to − 12.04°; t = − 48.15; df = 14; P < 0.001), indicating that postural change still produced a significant combined anteversion offset and that planning with standing parameters alone would underestimate the impingement risk of seated hip flexion with internal rotation.

Feasible solution space of preoperative dual-position simulation

Feasible solutions were obtained in all 15 cases under the four constraints of no impingement at 90° seated hip flexion, CA_sit 45°–65°, standing range of motion (maximum flexion ≥ 110°, maximum extension ≥ 20°), and FI_st ≤ 45° (Tables 3 and 4). Because these four criteria are entry conditions for candidate solutions and are therefore necessarily satisfied by the solutions returned by this workflow, the size of the feasible solution space, the constraint margins, and the distribution of bottleneck constraints better reflect the boundaries of applicability.

Table 3
Validation of dual-position range of motion (n = 15)

No.	No. of feasible solutions	Proportion satisfying constraints (%)	Minimum CA_sit distance from interval boundary (°)	Standing flexion reserve (°)	Standing extension reserve (°)	Bottleneck constraint
1	28	32.9	5.2	6.0	5.0	Avoidance of seated impingement
2	41	41.0	9.6	8.0	10.0	Avoidance of seated impingement
3	18	25.0	3.7	4.0	6.0	Seated combined anteversion
4	52	47.3	8.9	10.0	10.0	Avoidance of seated impingement
5	34	37.0	6.3	6.0	8.0	Avoidance of seated impingement
6	22	28.2	4.5	4.0	7.0	Seated combined anteversion
7	45	43.3	9.6	9.0	10.0	Avoidance of seated impingement
8	15	22.7	2.8	2.0	6.0	Seated combined anteversion
9	38	40.0	7.7	7.0	9.0	Avoidance of seated impingement
10	30	34.1	5.4	5.0	8.0	Seated combined anteversion
11	20	26.3	4.1	3.0	7.0	Seated combined anteversion
12	50	46.3	9.2	10.0	10.0	Avoidance of seated impingement
13	25	30.5	4.8	6.0	8.0	Avoidance of seated

Note: CA_sit, seated combined anteversion; candidate combinations were traversed in two tiers (first tier, 5° step coarse screening; second tier, 1° step refinement), and the denominator is the number of candidate combinations evaluated for that case; the bottleneck constraint is the constraint that eliminated the most combinations for that case.

No.	No. of feasible solutions	Proportion satisfying constraints (%)	Minimum CA_sit distance from interval boundary (°)	Standing flexion reserve (°)	Standing extension reserve (°)	Bottleneck constraint
						impingement
14	40	41.7	7.2	8.0	9.0	Avoidance of seated impingement
15	35	38.9	8.9	9.0	10.0	Avoidance of seated impingement
Mean ± SD	32.9 ± 11.6	35.7 ± 7.9	6.5 ± 2.3	6.5 ± 2.5	8.2 ± 1.7	—

Note: CA_sit, seated combined anteversion; candidate combinations were traversed in two tiers (first tier, 5° step coarse screening; second tier, 1° step refinement), and the denominator is the number of candidate combinations evaluated for that case; the bottleneck constraint is the constraint that eliminated the most combinations for that case.

Table 4
Feasible solution space and constraint margins for each case (n = 15)

No.	Seated maximum internal rotation at 90° hip flexion (°)	Standing maximum extension (°)	Standing maximum flexion (°)
1	52	25	116
2	55	30	118
3	51	26	114
4	58	30	120
5	53	28	116
6	52	27	114
7	56	30	119
8	50	26	112
9	54	29	117
10	53	28	115
11	51	27	113
12	57	30	120
13	53	28	116
14	55	29	118
15	56	30	119
Mean ± SD	53.7 ± 2.4	28.2 ± 1.7	116.5 ± 2.5

Note: The three indices were measured during preoperative dual-position simulation. The values shown for seated internal rotation are the maximum internal rotation achieved without impingement; the screening criteria were freedom from component or bony impingement at 30° internal rotation in 90° hip flexion, a minimum component clearance of ≥ 1 mm, standing maximum flexion ≥ 110°, and standing maximum extension ≥ 20° (these are screening entry criteria, not efficacy evaluation criteria).

The number of feasible solutions per case was 15–52 (32.9 ± 11.6), accounting for 22.7%–47.3% (35.7% ± 7.9%) of the candidate combinations evaluated for that case. Constraint margins were as follows: seated extreme internal rotation 53.7° ± 2.4° (minimum 50°); standing maximum flexion 116.5° ± 2.5° and maximum extension 28.2° ± 1.7°; CA_sit distance from the interval boundary 6.5 ± 2.3° (minimum 2.8°, case 8); and FI_st 34.5° ± 2.0° (maximum 39.9°) (Tables 2–4). In these patients with spinopelvic rigidity (FFA_sit 10.5°–25.5°), the rigid CA_sit constraint and the other three constraints could be satisfied simultaneously. Across the whole group, the bottleneck constraint was avoidance of seated impingement in 10 cases and CA_sit in 5 cases, indicating that avoidance of seated impingement and the CA_sit target interval are the main limitations on the applicability of this workflow.

Comparison between the individualized safe zone and the conventional safe zone

Postoperative CT-measured RA in this cohort ranged from 25.8° to 32.4° and MR-planned target RA from 26° to 35°; within the same anatomical coordinate system, both were consistently higher than the conventional static planning target of RA = 20° used in the prespecified analysis described in Section 1.3.2, indicating that individualized planning places the cup at appreciably greater anteversion than a conventional static target. RI ranged from 34° to 41° in the 15 patients. Because RI/RA in this study are derived from the anatomical CT coordinate system whereas the Lewinnek safe zone is defined by radiological angles on anteroposterior pelvic radiographs, the two cannot be directly converted quantitatively, and the comparison in (Fig. 5) is therefore qualitative only. The above proportions of non-fit are all preoperative three-dimensional simulation results and not actual postoperative clinical outcomes. Per the prespecified secondary analysis (section 1.3.2): if a uniform RA = 20° had been used, 46.7% (7/15) of patients would have had CA_sit < 45°; 33.3% (5/15) of patients could not simultaneously satisfy all seated functional constraints within the conventional safe-zone anteversion range, and although solutions within the safe zone existed in the feasible solution space of the remaining 10 cases, none was the optimal solution, so none was adopted.

Postoperative function and complications

The mean follow-up was 14.2 ± 2.5 months with no loss to follow-up. At the last follow-up, the Harris score had increased from 48.6 ± 10.2 preoperatively to 87.3 ± 5.1 (mean difference, 38.7; 95% CI, 35.6–41.8) and the Oxford score from 22.3 ± 6.8 to 40.8 ± 4.2 (mean difference, 18.5; 95% CI, 16.7–20.2); paired t-tests showed statistically significant differences (Harris $t = 26.86$, Oxford $t = 22.64$, both $df = 14$, $P < 0.001$), and the magnitude of improvement exceeded the respective clinically important improvement thresholds (Harris 15.9, Oxford 12.4). Because this was a single-center case series without a concurrent control group, functional improvement may have been influenced by rehabilitation training and the natural history of the disease, and the results are therefore presented descriptively only. No severe complications such as prosthetic dislocation, symptomatic impingement, periprosthetic fracture, or deep infection were observed during follow-up (0/15, one-sided 95% CI upper limit 18.1%). Given the limited sample size, this finding cannot exclude the risk of rare complications and does not demonstrate that this strategy reduces the incidence of dislocation or impingement. One patient after lumbar spinal fusion (case 1, FFA_sit 14.5°, RA 31°, CA_sit 50.2°) developed a mild limp 6 months postoperatively; CT showed normal prosthetic angles and the symptom resolved after rehabilitation training. Patient satisfaction was assessed at the last follow-up with a single-item question, “Overall, how satisfied are you with the result of your hip replacement?”, answered on a five-point Likert scale (very satisfied, satisfied, neutral, dissatisfied, or very dissatisfied); in line with the recommendations of the International Society of Arthroplasty Registries, patients who responded “very satisfied” or “satisfied” were classified as satisfied. On this basis, the satisfaction rate at the last follow-up was 93.3% (14/15).

Discussion

In this study, dual-position planning and an MR-assisted implantation workflow were implemented in 15 patients with spinopelvic rigidity, with a cup anteversion MAE of 1.68°; these results support further technical validation of this workflow. Spinopelvic kinematic studies have shown that in patients after lumbar spinal fusion, or with ankylosing spondylitis or severe lumbar degeneration, posterior pelvic tilt from standing to sitting is restricted, and even when the cup position lies within the safe zone, cup position mismatch may still occur in functional postures.[10–12] All 15 patients in this cohort had spinopelvic rigidity ($\Delta PT < 10°$), and the selected cup anteversion angles were consistently higher than the conventional static target of RA = 20° within the same

anatomical coordinate system (mean planned RA 29.4° ± 2.6°). Beyond pelvic posture, axial rotation of the femur in functional postures also alters combined anteversion.[8] Hardwick-Morris et al. showed that inter-individual variation in femoral axial rotation among THA patients is large, and functional femoral anteversion is not always consistent with CT-derived anatomical femoral anteversion.[8] FFA_sit varied markedly in this cohort (10.5°–25.5°), and the resulting CA_sit differed under the same cup anteversion, suggesting that cup planning should not adopt a uniform anteversion target divorced from femoral functional status[13]; although a larger head-neck ratio can increase the range of motion before neck-cup impingement, its effect is influenced by cup position and bony impingement. Pelvic postural change alters not only functional anteversion but also functional abduction; neglecting standing functional abduction and edge contact may increase liner edge loading and the risk of long-term loosening.[14] In this study, on the basis of achieving seated impingement-free motion, standing maximum flexion, maximum extension, and edge loading were further simulated, and all 15 cases met the preset thresholds, suggesting that dual-position balanced planning helps to accommodate both seated stability and standing mechanical safety.[15–16]

Mixed-reality technology provides a new path for individualized planning and intraoperative visualization in complex THA, and augmented-reality navigation helps to improve the accuracy of cup placement.[17] The value of this study is not simply improving static cup position accuracy, but integrating spinopelvic kinematics, femoral functional anteversion, and dual-position impingement-free simulation into preoperative planning and intraoperative guidance. The mean difference between planned and measured RA of − 1.31° indicates a constant systematic offset of approximately 1.3°, comparable in magnitude to the approximately 3° inherent placement error of imageless navigation systems,[18] and possibly arising from directionally consistent components such as registration error, orientation transfer error of the acetabular reamer and trial, and deviation in the impaction direction of the bone bed. Accordingly, the implanted angle was immediately verified by navigation intraoperatively in this study and readjusted if the error exceeded 3°; for cases in which the CA_sit margin from the 45° lower boundary was < 5°, this strategy recommends moderately raising the planned CA_sit target intraoperatively to reserve a safety margin to offset the risk posed by this negative systematic offset. This recommendation is an empirical, unvalidated suggestion based on observations in this cohort rather than a conclusion supported by the data of the present study. Postoperative CT verification confirmed the absence of an actual CA_sit falling into the functional risk zone, although its clinical significance still requires validation in larger populations with long-term outcomes. The difference between seated and standing combined anteversion in this cohort was statistically significant, indicating that planning with standing parameters alone would underestimate the impingement risk of seated hip flexion with internal rotation, which is the rationale for using seated combined anteversion as a rigid constraint in this study. The standing combined anteversion in this cohort was 39.2° ± 2.1°, also within the standing impingement-free interval recommended by that study (30°–50°), so both positions were in the low-impingement-risk zone. Unlike studies such as those by Vigdorchik and Pierrepont[7, 19], which focus mainly on correction of cup position for pelvic tilt, this strategy further incorporates seated femoral functional rotation into the baseline, uses seated combined anteversion as a rigid constraint, and adds standing edge-loading verification.

This study has several limitations. (a) It is a single-center, small-sample, single-arm case series (15 patients, level IV evidence) that included multiple causes of spinopelvic rigidity and had no concurrent control; it can only evaluate strategy feasibility and placement accuracy, cannot demonstrate superiority over conventional techniques, and cannot support etiological subgroup analysis; moreover, the small sample size (n = 15) limited statistical power, and caution is warranted when generalizing these findings. (b) The follow-up was only 14.2

months, lacking evidence on long-term outcomes such as prosthetic wear and loosening; the 45°–65° seated combined anteversion range is an exploratory cut-off from in vitro simulation and has not been validated in a large clinical cohort. (c) This strategy applies only to primary THA in patients with spinopelvic rigidity (as defined in Section 1.1) together with a standing-to-seated ΔPT < 10°, and depends on EOS equipment; it is subject to a systematic negative MR-navigation offset of − 1.31° that depends on CT-EOS registration accuracy (this offset was observed with our center's specific MR system in this cohort and should not be extrapolated directly to other MR/AR navigation devices). Bony simulation cannot reflect soft-tissue factors or replace intraoperative stability testing; as this was an exploratory descriptive analysis, no hypothesis testing for confirmatory inference was performed and no correction for multiplicity was applied; the Lewinnek safe zone can serve only as a qualitative reference: the prespecified assessment of safe-zone non-fit read the safe-zone limits within the anatomical coordinate system without conversion to radiological angles, and thus yields a conservative estimate rather than the true radiological non-conformity rate. Future work should prioritize verification of actual postoperative prostheses and functional postures, and evaluate the reproducibility and clinical value of this workflow in independent samples and controlled studies. (d) Satisfaction was captured with a single-item, five-point Likert question rather than a multi-item instrument; although this approach is recommended by the International Society of Arthroplasty Registries and is widely used in arthroplasty registries and large cohort studies, it yields only a global judgement and does not characterise the separate domains addressed by validated multi-item scales such as the self-administered patient satisfaction scale. A multi-item instrument, together with a concurrent control group, should be used in future studies.

Conclusions

An individualized cup placement strategy constrained by seated combined anteversion, with seated functional femoral anteversion fixed as the baseline, achieved satisfactory angular reproducibility of acetabular cup placement in patients with spinopelvic rigidity and a standing-to-seated ΔPT < 10°. Preoperative dual-position simulation indicated that the conventional static safe zone does not adequately cover the seated functional anteversion requirements of these patients. Short-term functional outcomes were satisfactory. This was a single-center, single-arm case series (level IV evidence); it can evaluate feasibility only and cannot establish superiority over conventional placement techniques, and the results require confirmation in larger, controlled studies with longer follow-up.

Declarations

Ethics approval and consent to participate

The study was conducted in accordance with the Declaration of Helsinki and its subsequent amendments, and all patients provided written informed consent.This study was approved by the Ethics Committee of Guizhou Hospital of Beijing Jishuitan Hospital (approval No. KT2019011001, approved on 10 January 2019). The study was conducted in accordance with the Declaration of Helsinki and its subsequent amendments, and all patients provided written informed consent.

Consent for publication

Written informed consent for publication was obtained from all patients.

Competing interests

The authors declare that they have no competing interests.

Funding

This work was supported by the 2025 Clinical Special Project of the Guizhou Provincial Department of Science and Technology (Qiankehe Chengguo LC [2025] General 163) and the 2025 Key Advantage Discipline Construction Project of the Guizhou Provincial Health Commission. The funding bodies had no role in the design of the study; in the collection, analysis and interpretation of data; or in the writing of the manuscript.

Author Contribution

Authors contributions GY and JS conceived and designed the study. GY, CL, PF and LD acquired the data. GY and ZK performed the statistical analysis and the three-dimensional simulations. GY drafted the manuscript. JS and ZJ critically revised the manuscript for important intellectual content. All authors read and approved the final manuscript and agree to be accountable for all aspects of the work.

Acknowledgements

Not applicable.

Data Availability

The datasets used and analysed during the current study are available from the corresponding author on reasonable request.

References

1. Lewinnek GE, Lewis JL, Tarr R, et al. Dislocations after total hip-replacement arthroplasties. J Bone Joint Surg Am. 1978;60(2):217–20.
2. Esposito CI, Gladnick BP, Lee YY, et al. Cup position alone does not predict risk of dislocation after hip arthroplasty. J Arthroplasty. 2015;30(1):109–13.
3. Abdel MP, von Roth P, Jennings MT, et al. What safe zone? The vast majority of dislocated THAs are within the Lewinnek safe zone for acetabular component position. Clin Orthop Relat Res. 2016;474(2):386–91.
4. Lazennec JY, Riwan A, Gravez F, et al. Hip spine relationships: application to total hip arthroplasty. Hip Int. 2007;17(Suppl 5):S91–104.
5. Buckland AJ, Puvanesarajah V, Vigdorchik J, et al. Dislocation of a primary total hip arthroplasty is more common in patients with a lumbar spinal fusion. Bone Joint J. 2017;99–B(5):585–91.
6. Heckmann N, McKnight B, Stefl M, et al. Late dislocation following total hip arthroplasty: spinopelvic imbalance as a causative factor. J Bone Joint Surg Am. 2018;100(21):1845–53.

7. Pierrepont J, Hawdon G, Miles BP, et al. Variation in functional pelvic tilt in patients undergoing total hip arthroplasty. Bone Joint J. 2017;99–B(2):184–91.
8. Hardwick-Morris M, Twiggs J, Kacker K, et al. Functional femoral anteversion: axial rotation of the femur and its implications for stem version targets in total hip arthroplasty. Arthroplast Today. 2022;18:16–23.
9. O'Connor PB, Thompson MT, Esposito CI, et al. The impact of functional combined anteversion on hip range of motion: a new optimal zone to reduce risk of impingement in total hip arthroplasty. Bone Jt Open. 2021;2(10):834–41.
10. Ike H, Dorr LD, Trasolini N, et al. Spine-pelvis-hip relationship in the functioning of a total hip replacement. J Bone Joint Surg Am. 2018;100(18):1606–15.
11. Esposito CI, Carroll KM, Sculco PK, et al. Total hip arthroplasty patients with fixed spinopelvic alignment are at higher risk of hip dislocation. J Arthroplasty. 2018;33(5):1449–54.
12. Stefl M, Lundergan W, Heckmann N et al. Spinopelvic mobility and acetabular component position for total hip arthroplasty. Bone Joint J. 2017;99-B(1 Suppl A):37–45.
13. Dorr LD, Malik A, Dastane M, et al. Combined anteversion technique for total hip arthroplasty. Clin Orthop Relat Res. 2009;467(1):119–27.
14. Elkins JM, Callaghan JJ, Brown TD. The 2014 Frank Stinchfield Award: the 'landing zone' for wear and stability in total hip arthroplasty is smaller than we thought: a computational analysis. Clin Orthop Relat Res. 2015;473(2):441–52.
15. Yoshimine F. The safe-zones for combined cup and neck anteversions that fulfill the essential range of motion and their optimum combination in total hip replacements. J Biomech. 2006;39(7):1315–23.
16. Hidaka R, Matsuda K, Nakamura M, et al. Optimal combined anteversion range for obtaining a wider range of motion without prosthetic impingement after total hip arthroplasty: a three-dimensional analysis study. J Orthop Surg Res. 2022;17(1):226.
17. Kanawade V, Dorr LD, Banks SA, et al. Precision of robotic guided instrumentation for acetabular component positioning. J Arthroplasty. 2015;30(3):392–7.
18. Fitzpatrick JM, West JB, Maurer CR. Predicting error in rigid-body point-based registration. IEEE Trans Med Imaging. 1998;17(5):694–702.
19. Vigdorchik JM, Sharma AK, Buckland AJ et al. 2021 Otto Aufranc Award: a simple Hip-Spine Classification for total hip arthroplasty: validation and a large multicentre series. Bone Joint J. 2021;103-B(7 Suppl B):17–24.

Figures

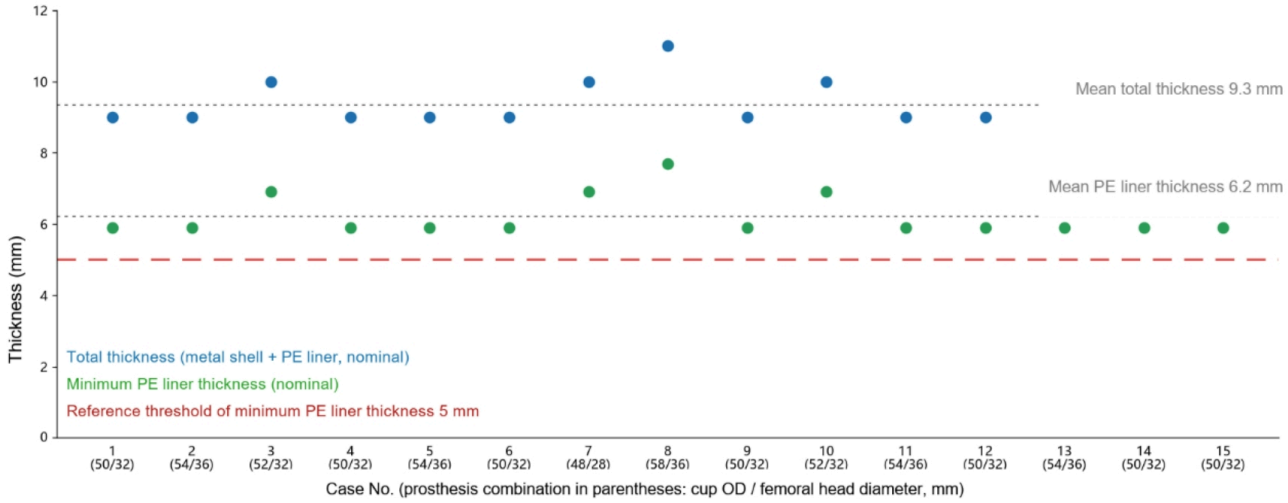


Figure 1

Total acetabular cup thickness and minimum PE liner thickness for different prosthesis combinations. Blue dots represent total acetabular cup thickness (metal shell plus PE liner), green dots represent minimum PE liner thickness, and the gray line indicates the group mean; the red dashed line is the minimum PE liner thickness threshold (5.0 mm); values in parentheses on the x-axis are prosthesis combinations (cup outer diameter/femoral head diameter, mm). Abbreviations: PE, polyethylene; MR, mixed reality

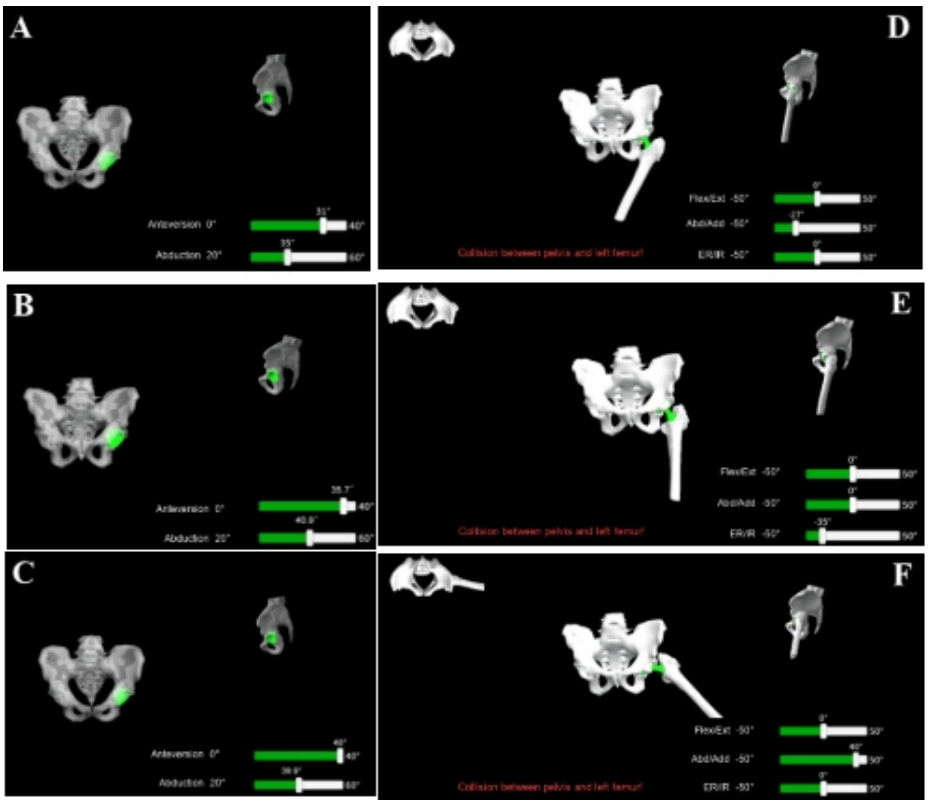


Figure 2

Representative case (male, 68 years, previous lumbar spinal fusion). A. Preoperative mixed-reality system interface: the virtual acetabular cup (green) is precisely registered to the patient's pelvic three-dimensional model, with anatomical cup abduction (RI) 35° and anatomical anteversion (RA) 31°. B. Seated functional cup anteversion (FA_sit) 35.7° and seated functional acetabular abduction (FI_sit) 40.9°. C. Standing functional acetabular abduction (FI_st) 39.9°. D–F. Assessment of seated hip range of motion. Abbreviations: RI, anatomical acetabular abduction; RA, anatomical acetabular anteversion; FA_sit, seated functional acetabular anteversion; FI_sit, seated functional acetabular abduction; FI_st, standing functional acetabular abduction; MR, mixed reality

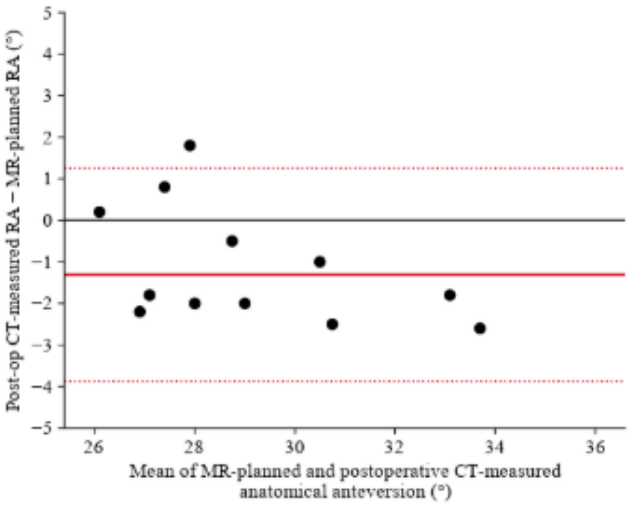


Figure 3

Bland–Altman agreement analysis between MR-planned and postoperative CT-measured RA (n = 15). d = postoperative CT-measured RA − MR-planned RA; the solid red line is the mean difference, the dashed red lines are the 95% limits of agreement, and the solid black line is the zero-difference reference line. Abbreviations: RA, anatomical acetabular anteversion; MR, mixed reality; CT, computed tomography

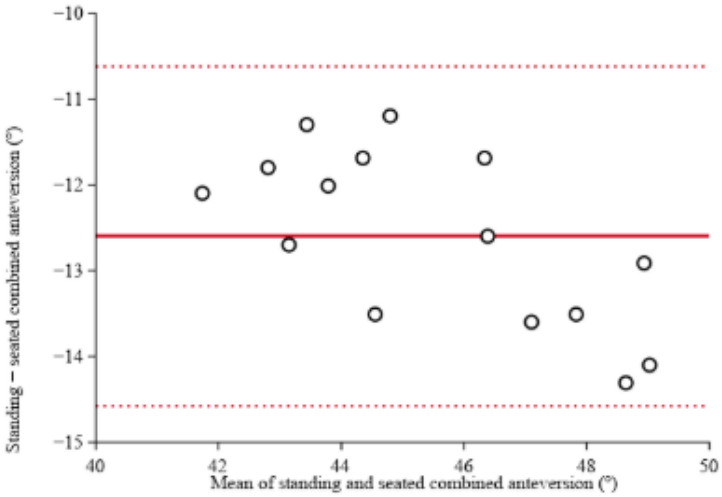


Figure 4

Paired difference plot of standing-to-seated combined anteversion offset (n = 15). The x-axis is the mean combined anteversion of the two positions and the y-axis is the offset (standing minus seated); the solid red line is the mean offset and the dotted red lines are the mean ± 1.96 × SD. Abbreviations: CA_sit, seated combined anteversion; CA_st, standing combined anteversion; SD, standard deviation

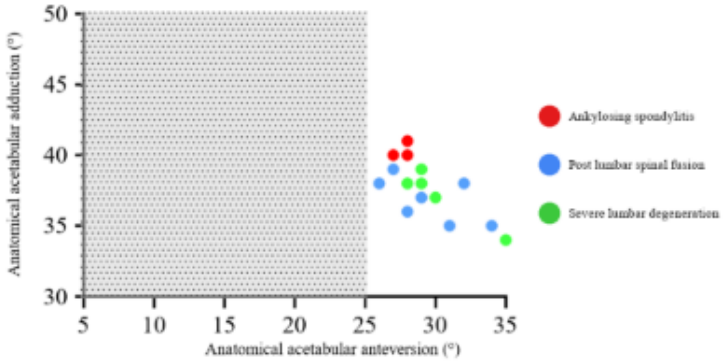


Figure 5

Scatter plot comparing individualized acetabular placement angles with the Lewinnek safe zone (n = 15). The gray area is the safe zone (anteversion 5°–25°, abduction 30°–50°); the x-axis is MR-planned RA and the y-axis is RI (Table 1); red indicates ankylosing spondylitis, blue previous lumbar spinal fusion, and green severe lumbar degeneration. The Lewinnek safe zone is defined by radiological angles on anteroposterior pelvic radiographs whereas RI/RA in this study are derived from the anatomical CT coordinate system, so the two cannot be directly converted quantitatively and this comparison is qualitative only. Abbreviations: RI, anatomical acetabular abduction; RA, anatomical acetabular anteversion; MR, mixed reality; CT, computed tomography